APPLIED GEOPHYSICS, Vol.7, No.1 (March 2010), P. 88 - 97, 15 Figures.
DOI:10.1007/s11770-010-0001-6

Instantaneous polarization filtering focused on suppression of surface waves*

Lu Jun[1], Wang Yun♦[2], and Yang Chun-Ying[1]

Abstract: The different characteristics of polarization of body and Rayleigh waves make it possible to separate these two types of waves by their characteristics and suppress the latter. The moving time-window analysis often is used in polarization filtering but it is difficult to determine a suitable time-window length, resulting in some problems, such as complex eigenvalues and non-convergence. For overcoming these disadvantages, in this paper, we introduce the concept of complex-trace analysis and conduct de-noise processing to suppress undesirable surface waves by instantaneous polarization analysis in the case of horizontal and vertical component seismic recordings from the Hauinan coal mine. The performance of the method is illustrated by examples with synthetic and field data and its effectiveness to remove surface waves from multi-component seismic data is demonstrated.
Keywords: Rayleigh waves, polarization, complex-trace, instantaneous polarization analysis, multi-component

Introduction

Low signal-to-noise ratio is one of the main problems in multi-component seismic data, especially with data acquired on land when only a single sensor is used to record the seismic signal. The cause is that the data are contaminated not only by random noise but also by other frequently encountered kinds of noise in geophysics (white and red). The noise may likely not be white (non-Gaussian, atmospheric disturbances, wind-induced pressure changes, standing or non-standing ocean pressure-waves on coasts, isotropic ambient seismic noise, and cultural noise) but coherent such as surface waves or multiple waves coupled to the target seismic signal. In these cases it is necessary to process the signal to remove this kind of noise. It is relatively easy to filter the random noise because of its obvious difference in frequency with respect to reflected signals. However, the elimination of Rayleigh waves is a more difficult task due to their large amplitudes and similar frequency content. This operation is particularly delicate with x-component records when using frequency filtering methods (Saatcilan and Canitez, 1988) because the converted (PS-) waves exhibit a low-frequency band compared with PP-waves (Wang et al., 2009). Hence we have decided to use seismic polarization analysis (Jurkevics 1988; Goebel, 1984).

As is well known, the Rayleigh waves have elliptic particle motion while the body waves are linearly polarized, so it is possible to distinguish Rayleigh waves from body waves in the seismic records through polarization analysis. Shimshoni and Smith (1964) and

Manuscript received by the Editor June 3, 2009; revised manuscript received December 25, 2009.
*This research is supported by the National Natural Science Foundation of China (grant No. 40574055), the National 973 Program (Grant No. 2006CB202207) and the Special Fund (Grant No. 2008ZX05035-001-003, 2008ZX05035-003-006HZ, 2008ZX05008-006-004).
1. Institute of Geology and Geophysics, Chinese Academy of Sciences, Beijing, 100029, China.
2. Institute of Geochemistry, Chinese Academy of Sciences, Guiyang, 550002,China.
♦ Corresponding author (Wang Yun, wangyun@mails.gyig.ac.cn).

White (1964) early made the separation of surface and body waves by polarization analysis using data from earthquakes and nuclear explosions. Benhama et al. (1988) introduced a filtering method based on seismic polarization analysis utilizing a moving time-window by which Rayleigh waves were filtered from body waves in multi-component recordings by calculating the eigenvalues of the covariance matrix and estimating the polarization ellipse. Many applications and improvements based on this method have been performed in the last two decades (Greenhalgh, et al., 1990; Bataille and Chiu, 1991; Cho, 1991; Cho and Spencer, 1992; Hendrick and Hearn, 1999; Wang and Teng, 1997). Perelberg and Hornbostel (1994) introduced weighting functions, although the method presents some problems when applied to field data: it is difficult to optimize a suitable time-window length to obtain real valued eigenvalues of the covariance matrix instead of complex values and the method cannot guarantee convergence in the eigenvalue computation. Also, noisy field data disturbs the particle motion and makes it difficult to obtain the linear or elliptic polarization.

Comparatively, complex trace analysis can provide instantaneous attributes without using time windows (René et al., 1986). Some researchers have proposed polarization filtering combined with complex trace analysis to obtain instantaneous attributes (Franco and Musacchio, 2001). Only one study has been done previously in China to successfully extract Rayleigh waves from real seismograms using the analytic signal method (Li et al., 1998). Chen et al. (2005) have carried out multi-window complex trace analysis to separate undesirable waves from natural earthquake signals.

However, these researches and results are all focused on de-noise filtering of natural earthquake and engineering seismic signals. In this paper, the complex trace analysis is improved and the instantaneous polarization filtering method is used to obtain instantaneous linear or elliptic polarization in the case of land multi-component records acquired in energy exploration. We have successfully overcome the problem that the overlapping frequency windows of Rayleigh waves and S-waves in x-component recordings make it difficult to clean the signals in the frequency domain using the moving time-window analysis in the filtering method.

Theoretical background

First, following the complex seismic trace analysis proposed by Taner et al., (1979), we let $x_r(t)$ and $z_r(t)$ be the x- and z-components of the seismic data input and the complex analytic signals are expressed by the equations

$$\begin{cases} X(t) = x_r(t) + ix_q(t) \\ Z(t) = z_r(t) + iz_q(t) \end{cases}, \tag{1}$$

where $x_q(t)$ and $z_q(t)$ are the Hilbert transforms of $x_r(t)$ and $z_r(t)$. Any of these functions $X(t)$ or $Z(t)$ is called the analytic signal or complex seismic trace and are widely used in seismic interpretation in petroleum exploration.

Second, in order to analyze the instantaneous polarization of each analytic seismic signal, the ellipticity $e(t)$ is defined as (Smith and Ward, 1974; René et al., 1986; Morozov and Smithson, 1996)

$$e(t) = \frac{b(t)}{a(t)}, \tag{2}$$

where $a(t)$ and $b(t)$ are the major and minor semi-axes of the polarization ellipse, respectively. If $e(t)$ is equal to 0, the soil particles move linearly or with linear polarity and if $e(t)$ is equal to 1, the particles describe a circumference, i.e., the particle motion has circular polarity. It should be noted that the ellipticity $e(t)$ at every sample must be smoothed to guarantee the stability of the filtering and the equation used for smoothing the ellipticity $e(t)$ is

Average ellipticity

$$\tilde{e}(t) = \frac{e(t-\Delta t) + e(t) + e(t+\Delta t)}{3}, \tag{3}$$

where Δt is the time step taken for computation. This average ellipticity is defined mainly to eliminate noise effects.

Finally, to suppress Rayleigh waves, it is necessary to establish a filtering function $G(t)$ corresponding to the ellipticity (Perelberg and Hornbostel, 1994) as:

$$G(t) = \exp\left(-\frac{\left(1 - \tilde{e}(t)\right)^2}{2\delta_e} \right), \tag{4}$$

where δ_e is the standard deviation of $\tilde{e}(t)$, which is a permissible error range of the ellipticities and can be calculated from all the $\tilde{e}(t)$ s by the statistical analysis. By using this standard deviation we can modulate filtering function $G(t)$ value for every trace until determining an optimum $G(t)$ value for suppressing the Rayleigh wave. Conventionally, if $G(t)$ is close to 0, the polarization is linear. If $G(t)$ is close to 1, the polarization is elliptic. Therefore, the Rayleigh waves in the x- and z- component seismic data can be identified by the $G(t)$ values and suppressed.

Synthetic example

The application of the method is illustrated starting from a 2-D layered earth model consisting of three near-surface layers and five underlying formations; their respective parameters are listed in Table 1. In order to simulate synthetic seismograms, we utilize 40 receivers in-line equally-spaced 20 m on the surface with the first of them at zero offset. Near-surface Rayleigh waves were numerically generated using the methods introduced by Knopoff (1964) and Schwab and Knopoff (1970) and PP- and PS-waves reflected in the deep layers are obtained by ray-tracing (Lu et al., 2006). Figure 1 shows the Rayleigh wave dispersion curve. Figure 2 displays synthetic single shot records containing the traces of the horizontal- and vertical-component ground motion, with S/N is 1. S/N is the ratio of reflection amplitude to Rayleigh wave amplitude.

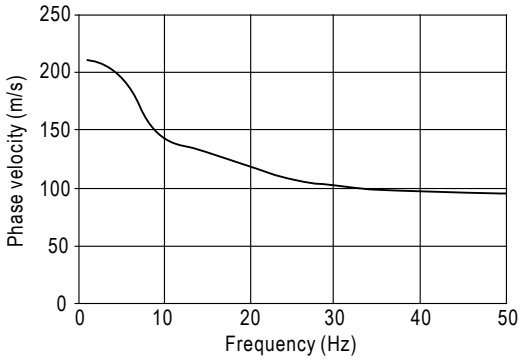

Fig.1 Theoretical phase velocity curve varying with frequency for the near-surface model Rayleigh wave.

Table 1 Model parameters

Formation		Depth (m)	P-wave velocity (m/s)	S-wave velocity (m/s)	Density (g/cm^3)	Dip in degrees	Reflections
Shallow layers	1	2	300	100	1.8	0	No reflections
	2	7	450	150	1.9	0	
	3	10	700	225	2.0	0	
Deep layers	4	1000	1250	800	2.8	-8	PP1, PS1
	5	2000	2500	1500	3.0	15	PP2, PS2
	6	2800	3200	1800	3.1	-12	Non-received reflection
	7	4000	3800	2000	3.2	10	PP4, PS4
	8	4500	4500	2600	3.4	0	No reflection in the bottom

Note: Positive dip is to the left and negative dip is to the right.

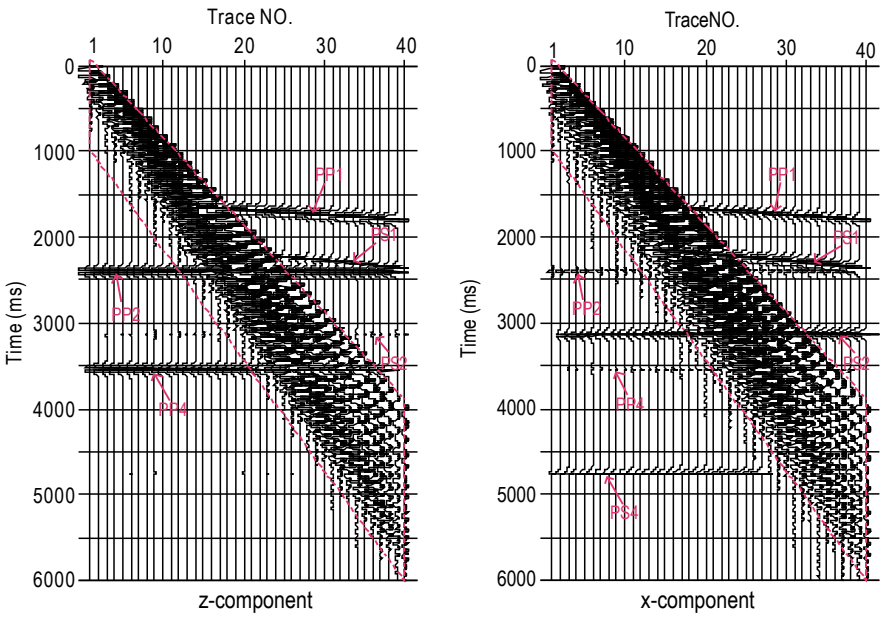

Fig. 2 Synthetic seismic data with S/N = 1.

As can be seen, the Rayleigh waves generated from the three shallow low-velocity layers appear as strong linear signals in Figure 2, whereas the body waves reflected from the deep layers appear as hyperbolic signals. There is a large energy-crossing area between body wave and surface wave signals in the time-space domain. The reflection generated by third interface cannot be detected at the surface due to the strongly dipping layers of the model and the short length of the linear array, so there are only PP and converted PS waves of the other deep interfaces. We have processed the synthetic data using the filtering function $G(t)$ at the window marked by the dashed line in Figure 2 with a $G(t)$ threshold value of 0.3 and standard deviation of 0.2. The synthetic data having $G(t)$ values larger than the 0.3 threshold must be multiplied by 0.1 to suppress the Rayleigh waves. The results obtained by digital filtering are shown in Figures 3 and 4. It is clear that the Rayleigh waves have been removed from the seismograms.

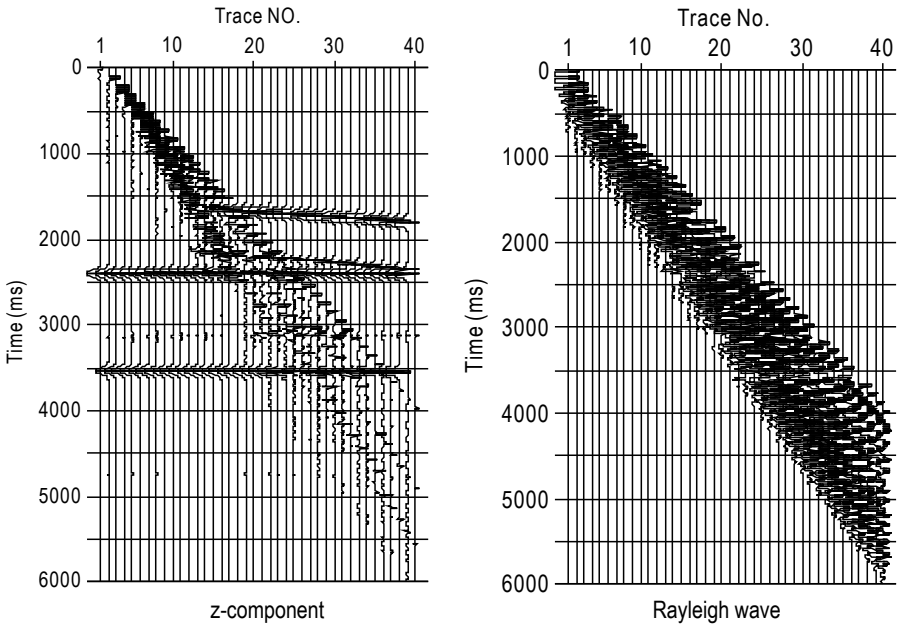

Fig. 3 Result obtained after filtering the z-component shown in Figure 2 by instantaneous polarization with *G*(*t*) threshold 0.3 and standard deviation 0.2.

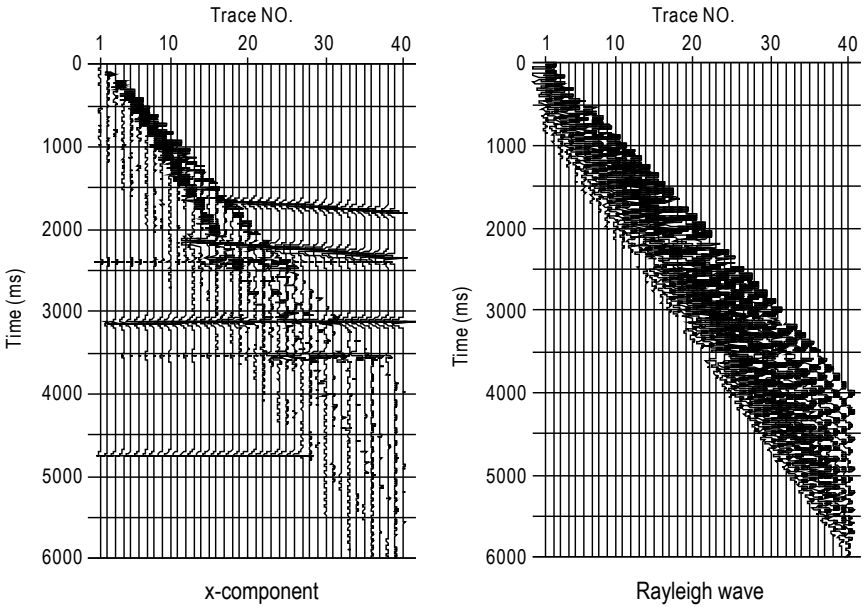

Fig. 4 Result obtained after filtering the x-component shown in Figure 2 by instantaneous polarization with *G*(*t*) threshold 0.3 and standard deviation 0.2.

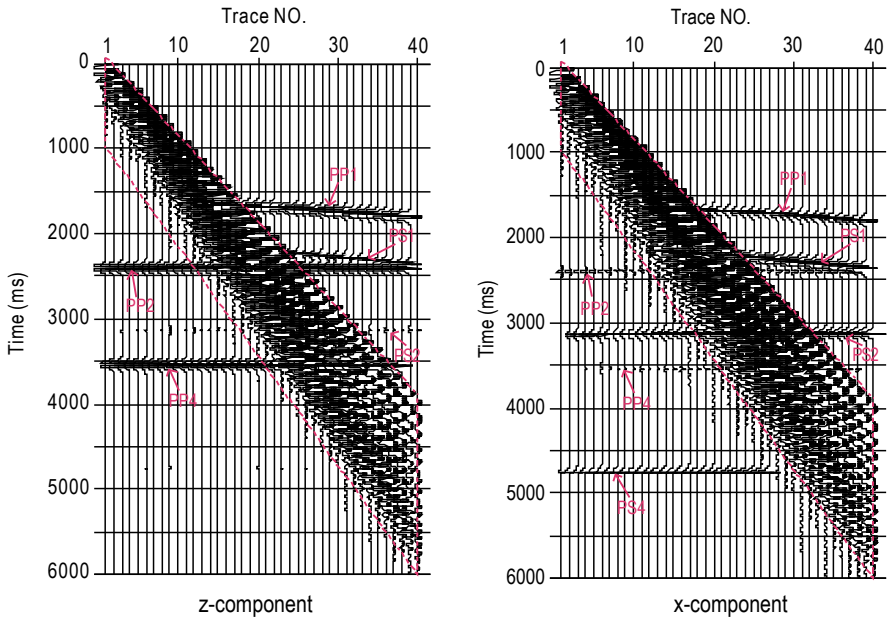

Fig. 5 Synthetic seismic data with S/N = 0.5.

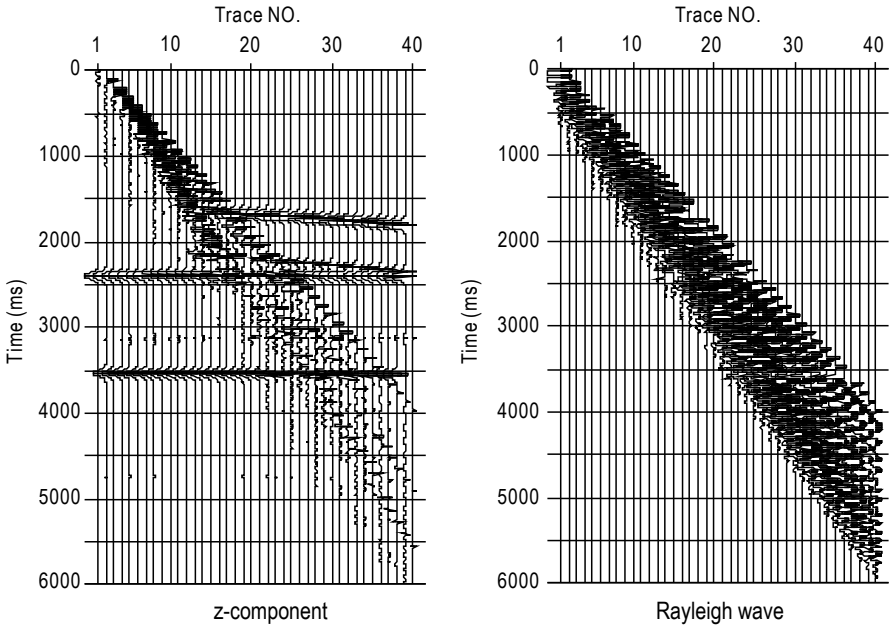

Fig. 6 Result obtained after filtering the z-component shown in Figure 5 by instantaneous polarization with $G(t)$ threshold 0.3 and standard deviation 0.2.

We also analyzed the effectiveness of the filtering method at different S/N ratios. The synthetic traces are shown in Figure 5 for S/N = 0.5 and in Figure 8 for S/N = 0.1. As can be seen from the filtering results shown in Figures 6, 7, 9, and 10, using the same $G(t)$ threshold and standard deviation, the filtering effect worsens with decreasing S/N. Figure 11 shows the curve $G(t)$for the 25th seismic trace at the time window of 2400-4000. So to determine a noise threshold above which the results are no longer satisfactory, the $G(t)$ in the overlapped area can be use as the standard. The instantaneous polarization filtering method utilizes the different polarization characteristics of body and surface waves to suppress the noise, so the method is applicable as far as the polarization characteristics of the body and surface waves are not changed. However, if the S/N is extremely small and the $G(t)$ values of the body

waves are over the threshold, the method does not provide a good result.

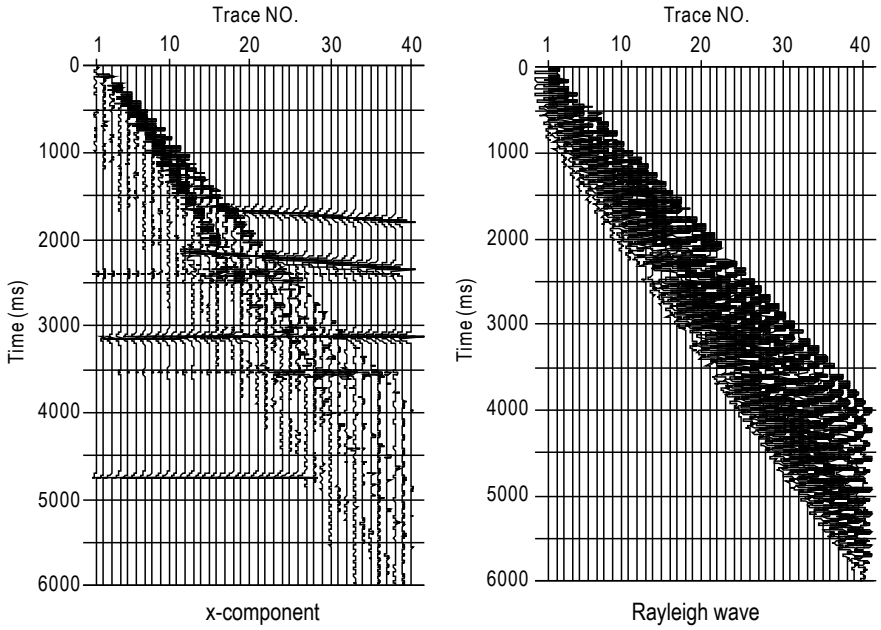

Fig. 7 Result obtained after filtering the x-component shown in Figure 5 by instantaneous polarization with $G(t)$ threshold 0.3 and standard deviation 0.2.

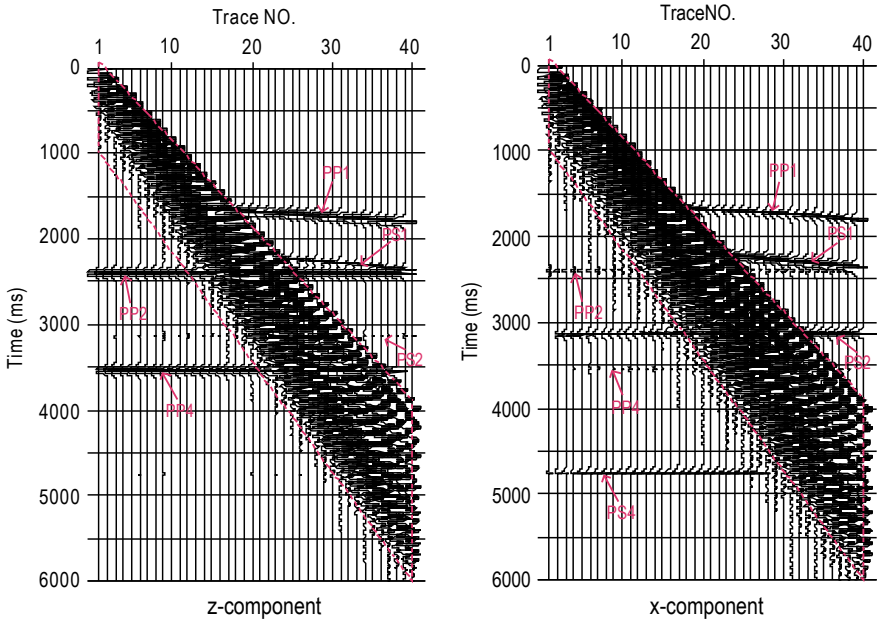

Fig. 8 Synthetic seismic data with S/N = 0.1.

Real data processing

We tested the method with 3D3C field data acquired in the Huainan coal mine area. There are five interesting coal seams over the depths of 700 m - 1000 m, corresponding to the PP reflection at 600 - 800 ms in the z-component section and the PS-wave reflections at 1400 - 1800 ms in the x-component section. The surface waves are from Quaternary sediments with a thickness up to 500 m and composed of interbedded clay sand, shale, and sand. Figures 12a and 13a show the recorded traces.

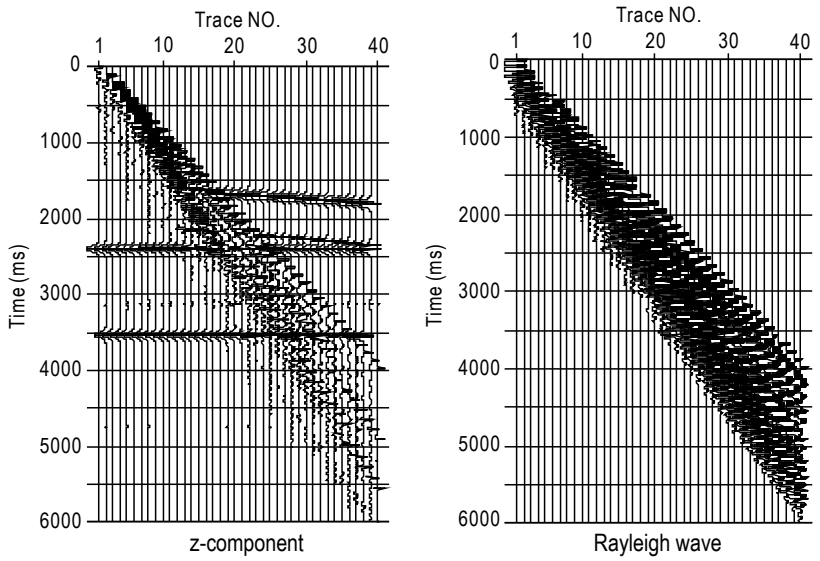

Fig. 9 Result obtained after filtering the z-component shown in Figure 8 by instantaneous polarization with $G(t)$ threshold 0.3 and standard deviation 0.2.

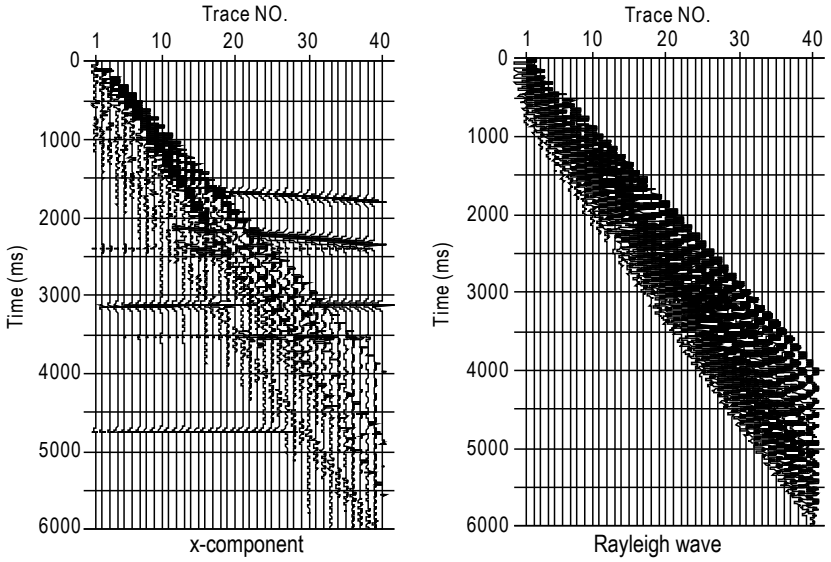

Fig. 10 Result obtained after filtering the x-component shown in Figure 8 by instantaneous polarization with $G(t)$ threshold 0.3 and standard deviation 0.2.

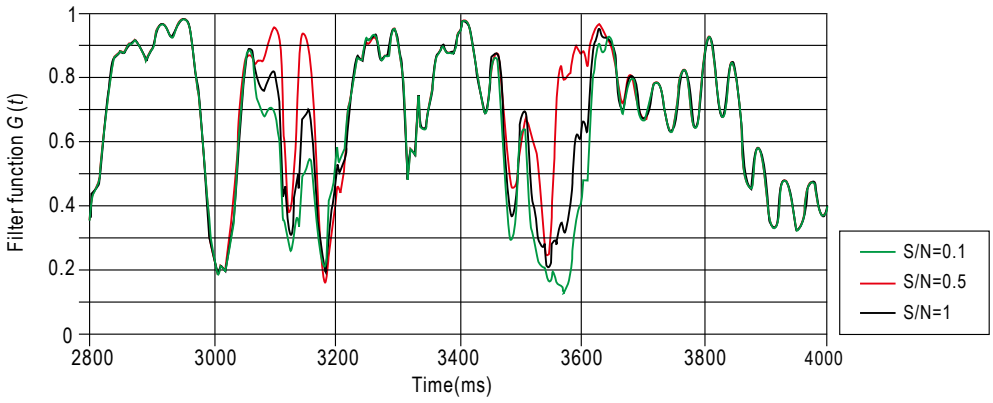

Fig. 11 Graphic representation of the function G curve for the 25th trace at different S/N (standard deviation is 0.2).

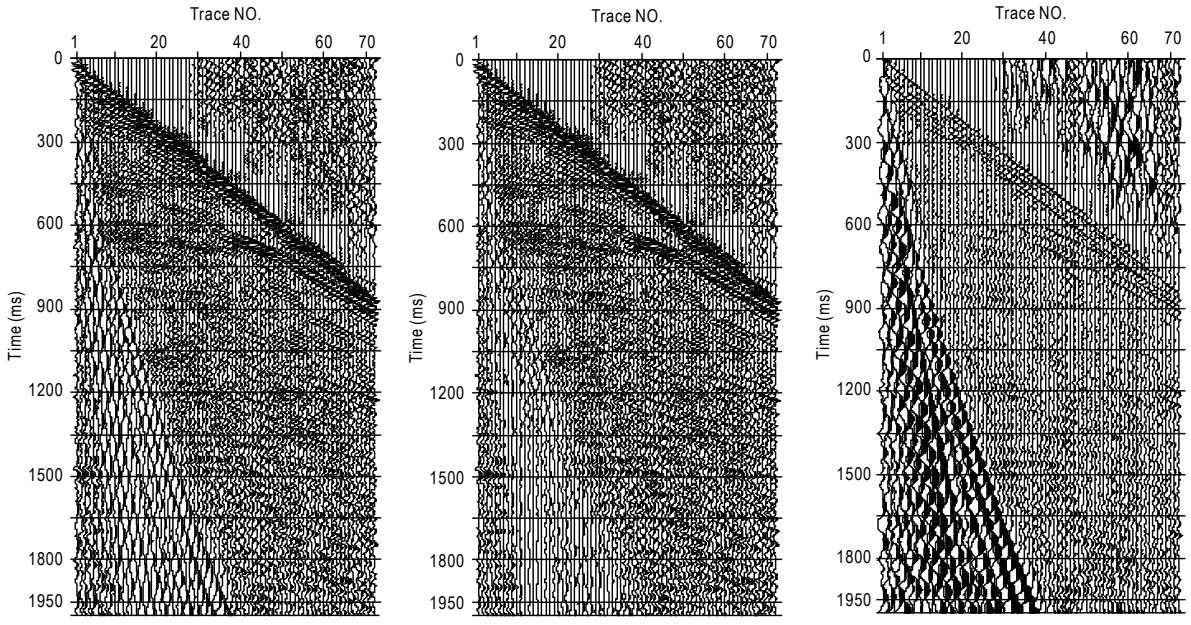

Fig. 12 Real z-component and filtered data by instantaneous polarization.

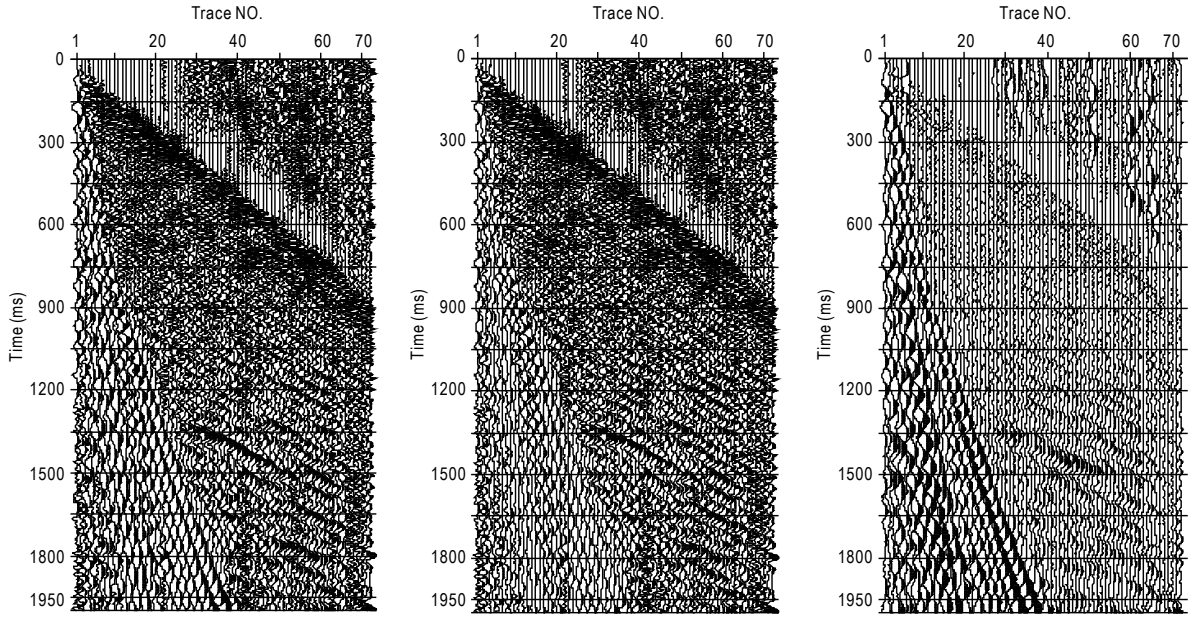

Fig. 13 Real x-component and filtered data by instantaneous polarization.

The results obtained after applying the instantaneous polarization filter can be seen in Figures 12b and c and 13b and c. It is obvious that the signal-to-noise ratio has been improved in both x- and z-components as a consequence of removing the Rayleigh waves from the seismograms. The performance of the filtering operations can be better understood if one sees the respective spectra obtained before and after filtering. The spectra from the z- and x-components of the Rayleigh waves are shown in Figures 14 and 15. In both cases the comparison of spectral amplitudes confirms that strong surface wave noise with elliptic polarization is eliminated in the low-frequency range so that the Rayleigh waves are basically removed from the field data while the amplitudes of the target signals are preserved by the filtering.

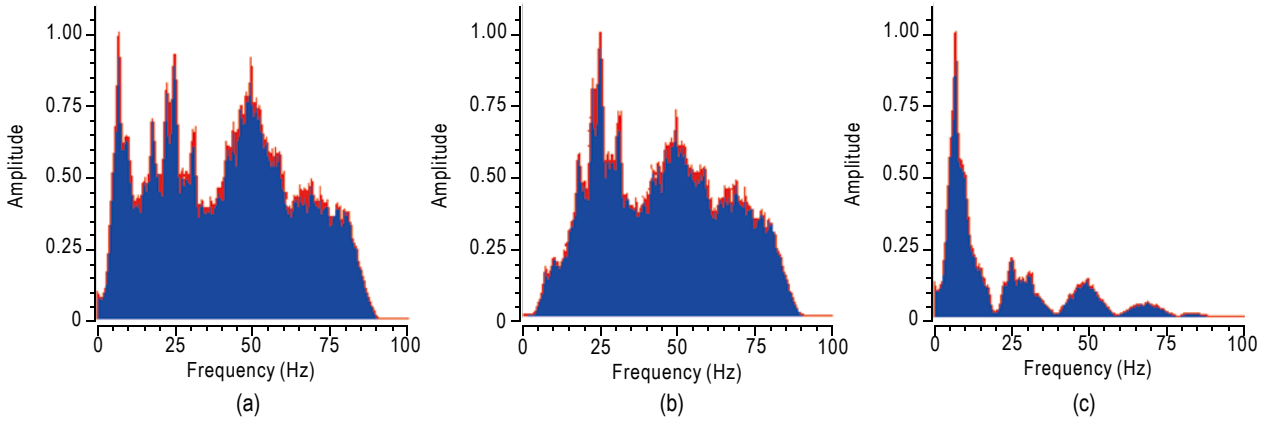

Fig. 14 Comparison of spectral amplitudes, (a) spectrum of the unfiltered z-component; (b) spectrum of the filtered signal; (c) noise spectrum.

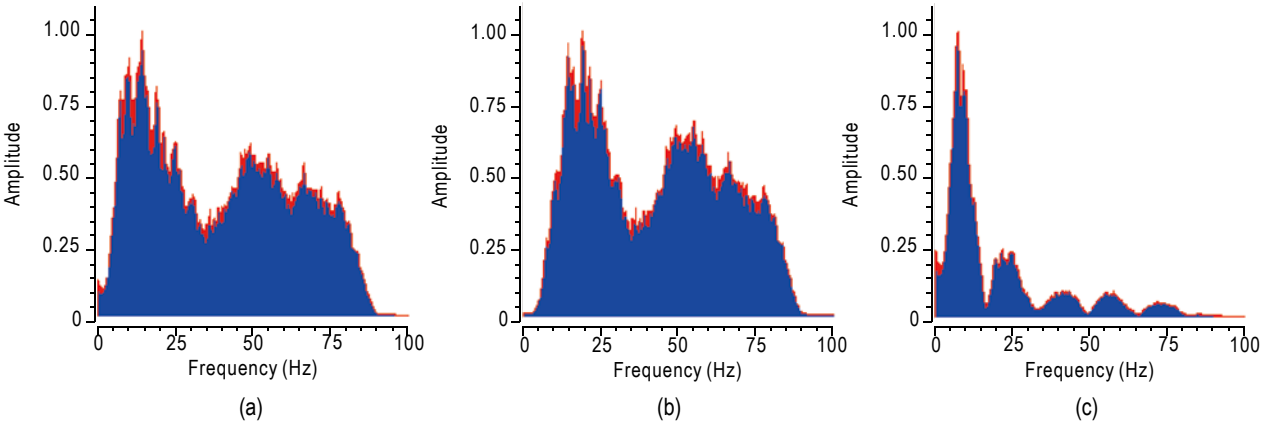

Fig. 15 Comparison of spectral amplitudes, (a) spectrum of the unfiltered x-component; (b) spectrum of the filtered signal; (c) noise spectrum.

Conclusions

The overlapping of Rayleigh waves and converted waves in the time-frequency domain and the low signal-to-noise ratio of seismic data make it difficult to separate these two kinds of waves in multi-component seismic exploration. The key in the filtering process of the converted wave is the suppression of the Rayleigh wave, without damaging the converted wave. The instantaneous polarization filtering proves to be an effective means to this end, able to deal with elliptic polarization. The selection of an optimum polarization filter is indeed important to suppress the Rayleigh wave to a point to be chosen after a series of tests and iterations to achieve better results.

Acknowledgements

The authors acknowledge Dr. G.M. Yu, for providing technical support to preprocess the PS-wave data .

References

Bataille, K., and Chiu, J. M., 1991, Polarization analysis of high frequency, three component seismic data: Bull. Seis. Soc. Am., **81**, 622 – 642.

Benhama, A., Cliet, C., and Dubesset, 1988, Study and applications of spatial directional filtering in three-component recordings: Geophysical Prospecting, **36**, 591 – 613.

Chen, Y., Zhang, Z. J., and Tian, X. B., 2005, Complex polarization analysis based on windowed Hilbert transform and its application: Chinese J. Geophys. (in Chinese), **48**(4), 889 – 895.

Cho, W. H., 1991, Decomposition of vector wavefield data: PhD Thesis, Texas A&M University.

Cho, W. H., and Spencer, T. W., 1992, Estimation of polarization and slowness in mixed wavefields: Geophysics, **57**, 805 – 814.

Franco, R., and Musacchio, G., 2001, Polarization filter with singular value decomposition: Geophysics, **66**(3), 932 – 938.

Goebel, V., 1984, Polarization and ground roll suppression: 54th Ann. Internat. Mtg., Soc. Explor. Geophys., Expanded Abstracts.

Greenhalgh, S. A., Mason, I. M., Mosher, C. C., and Lucas, E., 1990, Seismic wavefield separation by multi-component tau-p polarisation filtering: Tectonophysics, **173**, 53 – 61.

Hendrick, N., and Hearn, S., 1999, Polarization analysis: What is it? Why do you need it? How do you do it?: Exploration Geophysics, **30**, 177 – 190.

Jurkevics, A., 1988, Polarization analysis of three-component array data: Bull. Seism. Soc. Am., **78**(5), 1725 – 1743.

Knopoff, L., 1964, A matrix method for elastic wave problems: Bull. Seism. Soc. Am., **54**, 431 – 438.

Li, J. F., Li, R. H., and Wang, W. D., 1998, Study on the extraction of effective wave using analytic signal method in multi-component Rayleigh wave Exploration: Coal Geology & Exploration (in Chinese), **26**(2), 61 – 64.

Lu, J., Wang, Y., and Shi, Y., 2006, The best receiving window for acquisition of multi-component converted seismic data in VTI media: Chinese J. Geophys. (in Chinese), **49**(1) , 234 – 243.

Morozov, L. B., and Smithson, S. B., 1996, Instantaneous polarization attributes and directional filtering: Geophysics, **61**(3), 872 – 881.

Perelberg, A. I., and Hornbostel, S. C., 1994, Applications of seismic polarization analysis: Geophysics, **59**(1), 119 – 130.

Rene´, R. M., Fitter, J. L., Forsyth, P. M., et. al., 1986, Multi-component seismic studies using complex trace analysis: Geophysics, **51**(6), 1235 – 1251.

Saatcilan, R., and Canitez, N., 1988, A method of ground roll elimination: Geophysics, **53**, 894 – 902.

Schwab, F., and Knopoff, L., 1970, Surface-wave dispersion computations: Bull. Seism. Soc. Am., **60**, 321 – 344.

Shimshoni, M., and Smith, S. W., 1964, Seismic signal enhancement with three-component detectors: Geophysics, **29**, 664 – 671.

Smith, B. D., and Ward, S. H., 1974, On the computation of the polarization ellipse parameters: Geophysics, **39**, 867 – 869.

Taner, M. T., Koehler, F., and Sheriff, R. E., 1979, Complex seismic trace analysis: Geophysics, **44**, 1041 – 1063.

Wang, J., and Teng, T., 1997, Identification and picking of S phase using an artificial neural network: Bull. Seis. Soc. Am., **87**, 1140 – 1149.

Wang, Y., Lu, J., Shi, Y., et.al, 2009, PS-wave Q estimation based on the P-wave Q values: J. Geophys. Eng., **6**, 386 – 389.

White, J. E., 1964, Motion product seismograms: Geophysics, **29**, 288 – 298.

Lu Jun is a postdoc at the Institute of Geology and Geophysics, Chinese Academy of Sciences. He works for the Seismic Anisotropy, Multi-wave, and Multi-component Seismic Technique Research Group. His research work is mainly focused on the multi-wave processing method.